A Review of IGBT Models

Kuang Sheng, Barry W. Williams, and Stephen J. Finney

***Abstract*—In this paper, insulated gate bipolar transistor (IGBT) models published in the literature are reviewed, analyzed, compared and classified into different categories according to mathematical type, objectives, complexity, accuracy and speed. Features of the different models are listed. Different modeling criteria are discussed according to various circuit conditions, structures, thermal considerations and accuracies. Some problems and trends in IGBT modeling are discussed.**

***Index Terms*—IGBT, model, review.**

NOMENCLATURE

C_{cer}	Carrier redistribution capacitance (F).
C_{gs}	Gate-source capacitance (F).
C_{gd}	Gate-drain capacitance (F).
I_{sne}	Collector saturation current (A).
K_p	MOS channel transconductance (A/V^2).
L_e	Common emitter inductance (H).
N_f	Collector junction emission coefficient.
R_c	BJT collector resistance (3).
R_d	MOSFET drain resistance (3).
R_e	BJT emitter resistance (3).
t_{hl}	carrier high-level injection lifetime (s).
V_j	Anode junction voltage (V).
$V_{\rm MOS}$	MOS channel voltage (V).
V_{th}	Threshold voltage (V).
V_{base}	Conductivity modulated base voltage (V).
V_c	Collector voltage (V).
W_b	Base width (μm).
β_f	BJT forward current gain.
$\mu_{n,p}$	Electron (hole) mobility (cm^2/(V·s)).
BRM	Base resistance modulation.

I. INTRODUCTION

THE INSULATED gate bipolar transistor (IGBT) is an established replacement for the power bipolar junction transistor (BJT), Darlington transistor, metal oxide semiconductor field effect transistor (MOSFET), and GTO thyristor in medium frequency, medium power applications. As IGBT voltage and current ratings increase, its application range is extending to high power applications. Fabrication of a 5 kV device has been reported [1] and 3.3 kV, 1200 A devices are commercially available [2]. Structure design improvements of medium power IGBTs enable operation at higher frequencies. A 600 V, 50 A devices capable of hard-switching at 150 kHz is commercially available [3]. As a result of this pervasion, IGBT models are required by circuit designers and device manufacturers to predict circuit behavior, to understand device internal mechanisms and to improve structures.

Various circuit simulators including Saber, the simulation program with integrated circuit emphasis (SPICE) family, and some others are commercially available for IGBT modeling. The majority of IGBT models are used in one (or several) of these simulators. Based on the same core program, simulators in the Spice family (PSpice, Spice, HSpice, IG-Spice, Contec-Spice, SmartSpice, etc.) have different features for various applications. Saber is a comprehensive multitechnology circuit simulator which has strong program capability. Numerical simulators, including the SILVACO package and MEDICI, etc., are also available for IGBT device and circuit simulations. Although giving accurate results, they are not suitable for normal IGBT users because they require device manufacturing parameters and are costly and time consuming. However, these numerical simulation packages are useful for device manufacturers since they offer a reduced design cost and period.

Since the invention of the IGBT in 1982 [4], more than fifty papers have been published on IGBT models [1]–[68]. In modeling the IGBT, these papers use different methods and have different objectives, aspects and performance. In this paper, these IGBT models are reviewed, analyzed, and compared for different applications. Performance requirements for an IGBT model and existing problems are discussed.

II. IGBT MODELS

Most of the vertical IGBT models published in English since 1985 are listed chronologically in Table I. Authors and publication date of each model are indicated. Based on the modeling method used, the models are categorized into one of four different classes. Numerical models (finite element analyzers) are not included. A number ranging from one to five is assigned to each model to indicate complexity, with increasing complexity from one to five. Short comments describe the modeling method used, model features and achievements. Although the majority of models are developed for device users to simulate device behavior in circuits, some other models (mostly mathematical models) are developed for understanding device operation mechanism and for structure optimization.

A. Mathematical Models

The first category "mathematical," refers to analytical models based on semiconductor physics. Solving physics equations with different simplifications results in analytical

Manuscript received June 8, 1998; revised September 17, 1999. Recommended by Associate Editor W. M. Portnoy.

K. Sheng is with the Engineering Department, Cambridge University, Cambridge CB2 1PZ, U.K. (e-mail: ks280@eng.cam.ac.uk).

B. W. Williams and S. J. Finney are with the Department of Computing and Electrical Engineering, Heriot-Watt University, Edinburgh EH14 4AS, U.K. (e-mail: bww@cee.hw.ac.uk).

Publisher Item Identifier S 0885-8993(00)09796-9.

TABLE I
PUBLISHED IGBT MODELS FROM 1985 TO 1998

Metzner [25, 33]	1993, 1994	Semi-Numerical	4	Wide base region discretized to obtain accurate carrier behaviour for different conditions	Saber
Kvien, Undeland & Rogne [26]	1993	Semi-Mathematical	2	Not well described, incomplete	Krean
Hefner & Blackburn [30, 62]	1993	Mathematical	4	In addition to his models during 1988-1990, dynamic electrothermal behaviour included	Saber
Clemente & Dapkus *[21]*	1993	*Behavioural*	1	Curve-fitting method used, only for calculating switching losses in circuit design, no DC and dynamic behaviour	
Kim[1], Cho, Kim[2], Choi[2] and Han [27]	1993	Semi-mathematical	2	Simply combines Spice models of BJT and MOSFET, non-linear C_{gd} approximated polynomially	Spice
Andersson, Kuivalainen & Pohjonen [28]	1993	Semi-mathematical	3	Combines BJT and modified Spice level 3 models, non-linear C_{gd} and C_{ds} modelled hypobolically, no transient results given	Spice
Li, Lafore, Arnould & Reymond *[29]*	1993	*Mathematical*	3	Linear carrier distribution assumed, other aspects similar to Hefner's model	
Hefner [42]	1993	Mathematical	4	His previous model extended to PT-IGBTs	Saber
Kuo[2] & Chiang [31]	1994	Mathematical	4	For turn-on transient only, incomplete	
Goebel [34]	1994	Semi-Numerical	5	Combines one-dimensional numerical and analytical methods, difficult to implement into a normal circuit simulator	Saber
Kuzmin, Yurkov & Pomortseva [35]	1994	Mathematical	4	PT-IGBT analyzed, negative differential resistance modelled	
Kovac & Kovacova [37]	1994	Behavioural	2	Piece-wise modelling of C_{gd}	PSpice
Allard, Morel, Lin, Helali & Chante *[36]*	1994	*Mathematical*	4	Systematical modelling using bond graph method, implementation requires complex programming, accurate results given	PACTE
Besbes *[38]*	1995	*Mathematical*	4	Using bond graph method, similar to [36]	
Spanik, Dobrucky & Gubric [39]	1995	Mathematical	4	Equations from Hefner's model used, model with simplified form derived, reverse parallelled diode model included	

expressions describing carrier and electrical behavior. These expressions can be implemented into different simulators to emulate IGBT behavior for different applications.

Several early IGBT models were based on semiconductor physics. Turn-off behavior of the IGBT was first modeled by Baliga [5], [8] as a MOSFET driven PNP transistor, allowing the separation of the electron and hole current flow. In [6] the PNP-MOSFET configuration was validated quantitatively with discrete MOSFET and PNP transistors at turn-off, with a resistive load. Combining discrete MOSFET and PNP transistors is physically different from an IGBT. Tail current decay was assumed to be exponential and its time constant was expressed analytically. In addition to modeling tail current decay rate [6], Kuo *et al.* [7] gave an analytical expression for the forward conduction voltage taking into account of conductivity modulation in the base of both punch-through (PT) and non-punch-through (NPT) IGBTs. However, this model is not complete for circuit simulation because the MOSFET section, which is critical in transient simulation, has not been included. Fossum *et al.* [8] modeled a special

TABLE I (*Continued.*)
PUBLISHED IGBT MODELS FROM 1985 TO 1998

Mihalic, Jezernik, Krischan & Rentmeister [40]	1995	Semi-mathe matical	3	Modified MOSFET model used for DC characteristics, non-linear capacitance modelled piece-wisely	Spice
Alonso & Meynard [41]	1995	Semi-mathe matical	3	Short-circuit behaviour modelled with simple model	
Wong [43, 61]	1995, 1997	Behavi oural	1	Simply curve fitting for both static and dynamic characteristics, for system-level loss estimation in EMTP, not suitable for device behaviour simulation	EMTP
Udrea & Amaratunga *[44, 45, 64]*	1995 1997	*Mathe matical*	4	PiN diode effects on static characteristics of a T-IGBT are modelled by combination of PiN-BJT in series with MOSFET	
Feiler, Gerlach & Wiese *[47]*	1995	*Mathe matical*	5	Two-dimensional on-state carrier distribution is calculated analytically for D-IGBT, too complex for circuit simulation, suitable for device designers	
Kawaguchi, Terazaki & Nakagawa [48]	1995	Semi-mathe matical	2	Only for LIGBT which includes its special effects, not well documented	Spice
Petrie & Hymowitz [49]	1995	Semi-mathe matical	2	BJT-MOSFET configuration, non-linear C_{gd} modelled	Spice
Hsu[2] & Ngo [53]	1996	Behavi oural	3	Hammerstein configuration used, non-linear C_{gd} modelled	Saber
Musumeci, Raciti, Sardo, Frisina & Letor [51]	1996	Semi-mathe matical	2	Subcircuit model for PT-IGBT, controlled current source is used to model voltage dependent tail current	PSpice
Blaabjerg, Pedersen, Sigurjonsson & Elkjaer *[54]*	1996	*Behavi oural*	2	Curve-fitting power functions for loss estimations only	
Sheng, Finney & Williams [55]	1996	semi-mathe matical	1	Simple structure with BJT, MOSFET and a controlled current source for non-linear C_{gd}	PSpice
Monti [56]	1996	Behavi oural	2	Fuzzy based approach, non-linear C_{gd}, C_{gs} and C_{ds} modelled piece-wise	Matlab
Zhang, Watthanasarn & Shepherd [57]	1996	Semi-mathe matical	2	BJT-MOSFET combination, non-linear capacitances not modelled, not accurate enough for switching transient simulation	HSpice

lateral four terminal IGBT, which operates differently from a normal power IGBT.

Hefner [9], [11]–[15], [17], [18], [32] developed the first complete one-dimensional (1-D) analytical, charge controlled model suitable for circuit simulator implementation. Non-quasistatic effects (NQS), caused by the fast penetration of the space charge layer (SCL) edge, were considered in modeling the increase of inductive turn-off voltage. Nonlinear capacitances between terminals, which affect dynamic behavior, were also considered. The expression for the conductivity modulated base voltage is the same as that in [7], although in a simpler form. The model was extended to a punch-through structure and a dynamic electro-thermal model [30], [42]. Kraus *et al.* [19] modeled nonzero minority carrier concentration at the emitter edge of the base by averaging a sinusoidal lateral distribution. Dynamic carrier distribution was approximated by a polynomial. This model can only be implemented into complex circuit simulators such as Saber. The complete and complex mathematical model in [24], [50] gives complex equations for every model part including the wide-base PNP section, current in the SCL, the MOS channel section, capacitances, latch-up, the JFET effect, dynamic carrier behavior and dynamic electrothermal effects.

TABLE I (*Continued.*)
PUBLISHED IGBT MODELS FROM 1985 TO 1998

Amimi, Bouchakour & Maurel [58]	1996	Semi-mathe matical	3	BJT-MOSFET combination without non-linear capacitances, dynamic eletrothermal effects modelled	Saber
Yue, Liou & Batarseh [59]	1997	Mathe matical	3	Both high and low level injection considere, numerical methods used partly, not well documented	
Sheng, Finney & Williams [60]	1997	Mathe matical	5	Two-dimensional effects on devices static characteristics modelled analytically for D-IGBT	PSpice
Sunkavalli & Baliga [63]	1997	Mathe matical	3	Carrier enhancement effect on forward voltage drop (the same effect as in [60]) is modelled one-dimensionally for DI-LIGBT	
Strollo [65]	1997	Mathe matical	4	Carrier transport equation implemented by Laplace transform	PSpice
Napoli, Strollo & Spirito *[66]*	1997	*Mathe matical*	5	Two-dimensional on-state carrier distribution is modelled analytically for D-IGBT, finite carrier lifetime considered, too complex for circuit simulation, suitable for device designers	
Sigg, Tuerkes & Kraus [67]	1997	Mathe matical	4	Complex model accounting for dynamic carrier distribution and dynamic electrothermal behaviour	Saber
Ammous, Allard & Morel *[68]*	1998	*Semi-mathe matical*	2	Thermal modelling only	PACTE

Note: Different authors with the same surname are superscripted 1, 2, etc.

The bond graph method [36], [38] was used to model bipolar power semiconductor devices including the IGBT. Although giving accurate results, these models impose higher implementation requirements on the simulator. An important feature of the IGBT, namely, the enhancement of base conductivity modulation resulting from the accumulation layer under the gate, was modeled with a P-i-N diode for a Trench IGBT (TIGBT) [44], [45], [64]. This effect was noticed in [19]. The same effects were modeled for a normal DIGBT by Sheng *et al.* [60] by solving the two-dimensional (2-D) carrier distribution equations. This model gives a close-formed expression for the forward conduction voltage, and can be used in both circuit simulation and device analysis. These same effects were also modeled for a lateral IGBT (LIGBT) [63]. The static 2-D carrier distribution was expressed in series form by Feiler *et al.* [47] and Napoli *et al.* [66]. Infinite diffusion length was assumed in [47] while finite carrier lifetime (thus diffusion length) was considered in [66]. Among the four models described above, although only the one in [60] is suitable for both circuit simulation and optimizing IGBT structures, all the four are useful in understanding IGBT operating mechanisms. In [65], Laplace transforms of the carrier transport equations were implemented directly into an electrical subcircuit to model the IGBT. This method compromises between accuracy and easy of implementation. Results are insufficient to prove overall accuracy of the model. No significant difference has been found between the models in [28], [39] and the Hefner model.

B. Semimathematical Models

The second IGBT modeling category is "semimathematical." Such models are partly based on physics while combining existing models (in the Spice family, Saber, etc.) for other components.

Aimed at simplicity, most of the models in this category connect existing MOSFET and BJT models in a circuit simulator while using other parts to account for some specific effects in an IGBT. These specific effects include base conductivity modulation, nonlinear capacitances between terminals, nonquasistatic (NQS) effects, voltage dependent current tail, carrier lifetime dependent voltage increase rate at turn-off, conductivity modulation lag at turn-on, etc. In [16], [20], a modified Ebers–Moll model was used for the BJT and fixed capacitance was used to account for the NQS effects proposed by Hefner [9], [11]–[15], [17], [18], [32]. Piecewise values were given to the MOSFET gate-source and gate-drain capacitances. These nonlinear capacitances can be modeled physically [23], [49], [55], polynomially [27], hypobolically [28], and piece-wisely [40]. In [48], a lateral IGBT was modeled by Kawaguchi *et al.*which considered the special P-channel induced in the substrate. In [51], the voltage dependent current tail was modeled by a controlled current source while in [57] and [58], none of these effects were taken into account. An IGBT model was also proposed by Kvien *et al.* [26] which combined two diode models and MOSFET

TABLE I (*Continued.*)
PUBLISHED IGBT MODELS FROM 1985 TO 1998

Author(s)/paper(s)	Year	Type	Comp lexity	Comments	simula-tor
Baliga *[5, 8]*	1985, 1987	*Mathe matical*	4	PiN(BJT)-MOSFET connection used for static characteristic, tail current analyzed	
Kuo[i], Choi[i], Giandomenico, Hu, Sapp, Sassaman, & Bregar *[6, 7]*	1985, 1986	*Mathe matical*	4	One-dimensional closed-form static on-state voltage (V_F) solved, tail current decay rate calculated	
Hefner [9, 11-15, 17, 18, 32]	1988-1990	Mathe matical	4	Comprehensive one-dimensional model for both static and dynamic characteristics, good transient accuracy,	Saber, PSpice, etc.
Fossum, McDonald & Shibib [10]	1988	Mathe matical	3	For LIGBT, very low power results given	Spice
Shen & Chow [16, 20]	1991, 1993	Semi-mathe matical	2	Simple combination of Spice BJT and MOSFET model with piece-wise approach for non-linear gate capacitances (C_{gs}, C_{gd})	Contec-Spice
Kraus & Hoffmann [19]	1993	Mathe matical	4	Static carrier equations solved two-dimensionally, transient carrier behaviour approximated, for NPT-IGBT only, infinity base lifetime assumed	Saber
Fatemizadeh, Tchouangue & Silber [24, 50]	1993, 1996	Mathe matical	5	Complex expressions for DC characteristics, carrier dynamics approximated with Galerkin method, Dynamic electrothermal behaviour included	PSpice
Tzou & Hsu[l] [22]	1993	Behavi oural	2	Curve-fitting method used for non-linear behaviour, except for MOSFET	Spice
Protiwa, Apeldoorn &Groos [23]	1993	Semi-Behavi oural	2	Combining PSpice BJT and MOSFET models, base resistance and non-linear C_{gd} included	PSpice

channel resistance. However it was not well described and insufficient results were presented.

All of the models discussed in this category can be used by a circuit simulator such as Saber or one in the Spice family. They are not as accurate as mathematical models, because the wide base BJT in the IGBT does not resemble any of the existing discrete power BJTs models.

C. Behavioral Models

The third model category is "behavioral" or "empirical." These models simulate IGBT behavior without considering their physical mechanism. Measured IGBT characteristics are fitted by different methods. The resultant expressions, databases or components are then used in a simulator to model the IGBT.

In [22], IGBT output characteristics were modeled by a resistor and current source. The resistance values, source current and nonlinear capacitances were obtained from a look-up table. Curve fitting methods were used in the models in [21] and [54] for estimating IGBT losses. No static and dynamic characteristics can be predicted with these two models. Although the model proposed by Wong [43], [61], which stores static and dynamic characteristics in a database, can be used in the electromagnetic transient program (EMTP) for circuit simulation and loss estimation, it is not suitable for predicting IGBT circuit behavior. Behavior of the IGBT was also modeled with a fuzzy logic approach by Monti [56]. Reasonable results were given but this model was not well described. The IGBT was treated as a nonlinear system which was identified by the Hammerstein configuration in [53]. Special characteristics of the IGBT, which were mentioned in the previous sub-section, are normally not modeled with models in this category.

D. Seminumerical Models

The last IGBT model category is referred to as "semi-numerical." In these models, different to the compact models discussed in previous sub-sections, finite element methods are used to model the wide base while the other device parts are modeled

by earlier analytical methods. Because of the complexity and difficulty in modeling IGBT base, numerical methods were employed in some models to describe it accurately. In [25], [33], the ambipolar diffusion equations were solved numerically in the discretized base. Together with mathematical models for other parts, the results were used to describe IGBT behavior. The same method was also used by Goebel [34]. Accurate transient results have been shown, at the cost of speed and computational effectiveness. Although the models in this category have been implemented into Saber, they are inconvenient for implementation into normal circuit simulators.

As described in this section, many models have been developed to describe the behavior of an IGBT in different environments. Because of the diversity of IGBT simulation environments, each model type has its own particular niche, as discussed in the next section.

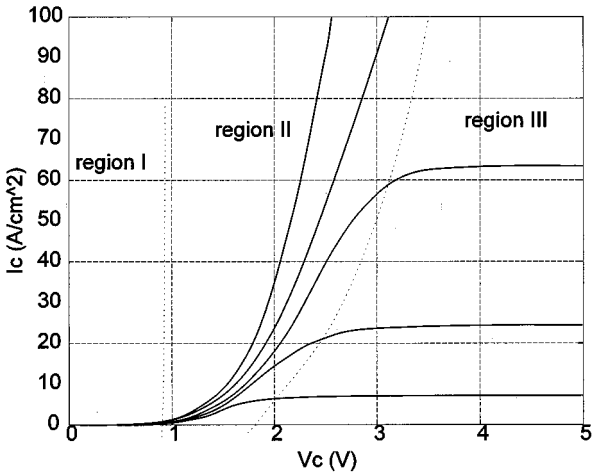

Fig. 1. Typical output characteristics of an IGBT.

III. IGBT Behavior and Requirements of a Model

In this section, behaviors of the IGBTs at steady-state, in switching circuits with different topologies and under short-circuit conditions are explained briefly. The effects of structure and temperature (static and dynamic) on their behavior are discussed. In order to model IGBT behavior accurately under these various circumstances, different requirements and aspects are necessary in a model. These criteria are highlighted and explained.

The effects of simulation accuracy and speed requirements for different model applications on the selection of the IGBT model are also discussed.

A. Static Characteristics

Typical IGBT output characteristics are shown in Fig. 1. The IGBT on-state voltage is made up of three components; anode junction voltage (V_j, including the buffer-base junction voltage in case of PT IGBT), conductivity modulated base voltage (V_{base}) and MOS channel voltage ($V_{\rm MOS}$).

Junction voltage variation is only noticeable at very low current density and can be modeled adequately by the classical P-N junction voltage expression. It should be noted that the voltage drop on the buffer-base junction is negative when the IGBT is forward conducting.

The output characteristics with a sufficiently high gate bias are the main interest when calculating device conduction loss during normal operation. Then, the device operates in region II of Fig. 1 and the base voltage (V_{base}) contributes significantly to the total voltage. In order to model V_{base} accurately, the excess carrier distribution and conductivity modulation in the base have to be calculated. These were modeled in [7], [9], [11]–[15], [17], [18], [32], [36], [44], [45], [64], and [60]. It was also demonstrated that two dimensional effects have to be considered for the Trench IGBT (TIGBT) [44], [45], [64] and the DMOS IGBT (DIGBT) [60]. Otherwise, V_{base} is overestimated and longer carrier lifetime and/or smaller MOS channel voltage is needed to fit the correct IGBT voltage. Accurate modeling of V_{base} requires consideration of two dimensional effects, carrier distribution, accurate mobility modeling including carrier-carrier-scattering and the band-gap-narrowing effect in the heavily doped collector. The resultant complex equations were approximated in many of the models listed, according to the accuracy required. In the Hefner model [9], [11]–[15], [17], [18], [32], [43], the base width (W_b), base carrier lifetime (t_{hl}), carrier mobilities ($\mu_{n,p}$) and collector junction saturation current (I_{sne}) are especially important for base voltage calculation. The base voltage is simply included in the BJT collector resistance (R_c, or emitter resistance R_e) or the MOSFET drain resistance (R_d) for many semi-mathematical models, where BJT forward current gain (β_f) is also important.

The MOSFET channel dominates IGBT behavior in region III of Fig. 1. It also contributes significantly in region II. The channel transconductance (K_p, accounting for the channel width and channel length) and the threshold voltage (V_{th}) are two basic parameters in modeling channel static characteristics. Accurate modeling of these two regions requires a model accounting for channel effects such as channel length modulation, velocity saturation, electric field dependent mobility, doping concentration gradient and subthreshold current. Parameters critical in modeling these specific channel effects are different in various simulators. Complex models for the MOSFET channel are presented in [16], [24], [28], [69] and many other MOSFET modeling papers [70]. The four levels for the MOSFET model in PSpice and those in Saber provide good channel accuracy in most applications.

Forward and reverse breakdown characteristics (of some NPT IGBTs) are modeled in Hefner's model and some others [24], [50], [35], [49].

B. Dynamic Characteristics

As a power semiconductor switch, the dynamic characteristics of the IGBT receive particular attention. In the following paragraphs, the requirements and behavior of IGBT models are discussed in different circuit conditions. As examples, the behavior of two models, the Hefner model [9], [11]–[15], [17], [18], [32], [43] (***model 1***) and a semi-mathematical model [55] (***model 2***), are compared with experimental data. The Hefner model is a physics based mathematical model which is implemented into Saber and some commercial circuit simulators in the Spice family. The semi-mathematical model [55] combines

existing MOSFET and BJT PSpice models while considering nonlinear capacitances to improve transient characteristics. Most of semi-mathematical models listed in Section II, [16], [20], [23], [27], [28], [40], [49], [51], [55] use this method but differ slightly. These models are widely used by users and manufacturers including International Rectifier (IR).

Because of the fast switching speed of the IGBT, circuit parasitic components (such as stray inductances) have significant effects on IGBT electrical behavior. The gate drive circuitry is also important. Therefore these circuit parameters have to be correctly accounted for before model accuracy can be evaluated. It is also found that turn-on behavior of an IGBT with a clamped inductive load is dominated by the associated free-wheel diode [79]. Therefore, in order to avoid complication, waveforms of hard-switching turn-on are not included in the following discussion.

1) Clamped Inductive Load: Clamped inductive load conditions occur in inverter bridge circuits, converter circuits (buck, boost and Cuk) and chopper circuits, with an inductive load. The vast majority of IGBTs are designed for and are used under such a load condition.

a) Hard-switching turn-off: Most IGBTs are used in a hard-switching configuration because of the associated simple circuit topology which means low cost. Furthermore, IGBTs are normally optimized by manufacturers for such conditions. Parts a and b of Fig. 2 show turn-off waveforms of two IGBTs, with a PT (IRGP440U) and NPT (BUP304) structure, respectively. It is obvious that the two technologies result in significantly different electrical behavior. Note that IGBT "collector" refers to "anode" and "emitter" refers to "cathode."

The turn-off period can be divided into five intervals as labeled on the PT IGBT waveforms in Fig. 2(a). Similar intervals and gate waveforms exist for the NPT IGBT.

Interval t_1 to t_2: The gate capacitance discharges, following the turn-off gate signal. The decrease rate is determined by the gate voltage source dv/dt and the discharge circuit time constant, which is dependent on gate-source capacitance (C_{gs}), gate-drain capacitance (C_{gd}) and gate resistance.

Interval t_2 to t_3: The gate voltage is held at a constant value (V_{pl}) so that the internal gate bias is just sufficient to keep the IGBT conducting the load current. The collector voltage increases slightly during this period and the duration is dominated by C_{gd}

Interval t_3 to t_4: The collector voltage increases quickly, with the space charge layer (SCL) edge extending toward the collector (anode) junction. To improve understanding of the IGBT (PT and NPT) behavior that follows, the dynamic evolution of minority carriers in the base, created by a 2-D numerical simulator, is illustrated in Fig. 3. It can be seen that as the SCL expands, carriers are removed from the base. However, because the collector current is unchanged before t_4, carrier distribution in most of the undepleted base is only slightly changed for the NPT IGBT. The stored electrons are provided by the channel current (if it has not vanished completely), and are removed through recombination in the base and injection into the collector. Therefore, their decrease rate, thus the collector voltage increase rate, is dependent on base carrier lifetime, collector structure and gate drive condition.

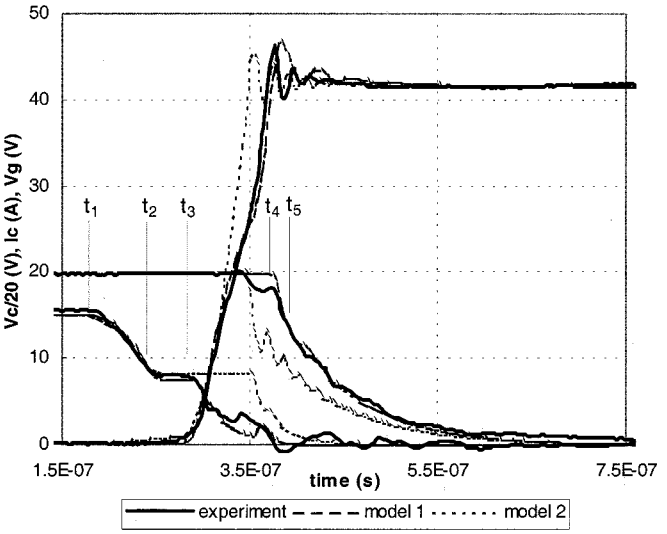

(a)

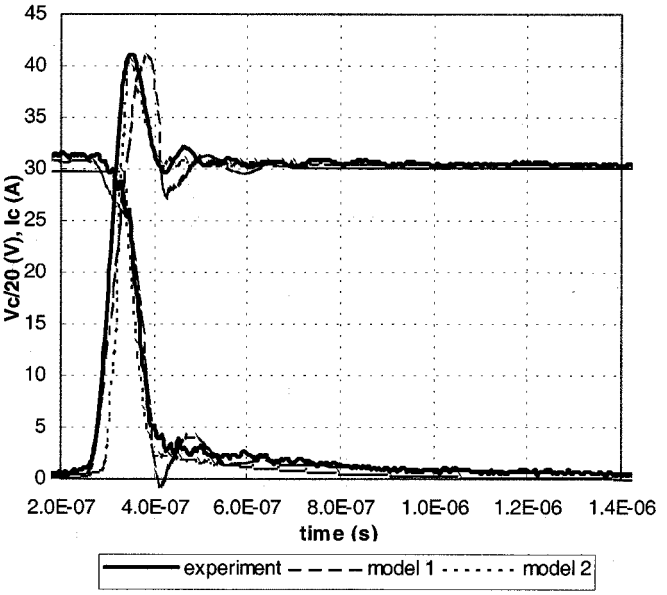

(b)

Fig. 2. Turn-off waveforms for (a) PT IGBT and (b) NPT IGBT.

Interval t_4 to t_5: The collector current falls to a value which is only dependent on the device. The rate of current fall, which determines collector voltage overshoot magnitude, is also dependent on base carrier lifetime as well as the gate circuitry. After t_5, the remaining carriers in the base decay, producing the so called tail current.

Accurate modeling of IGBT behavior after t_3 necessitates correct modeling of MOS capacitances, mobile charge in the SCL, base charge and collector structure effects. Model parameters used to model the hard-switching behavior are listed in Table V for both models 1 and 2 in the Appendix. Several specific IGBT features are worth noting. The voltage rise phase (t_3–t_4) of a PT IGBT has an unusual shape which shows a decrease in dV_c/dt followed by a fast increase [76]. The decrease in dV_c/dt is caused by the high carrier concentration in the vicinity of the N–N$^-$ junction while the subsequent fast increase is because no carrier removal occurs after the elec-

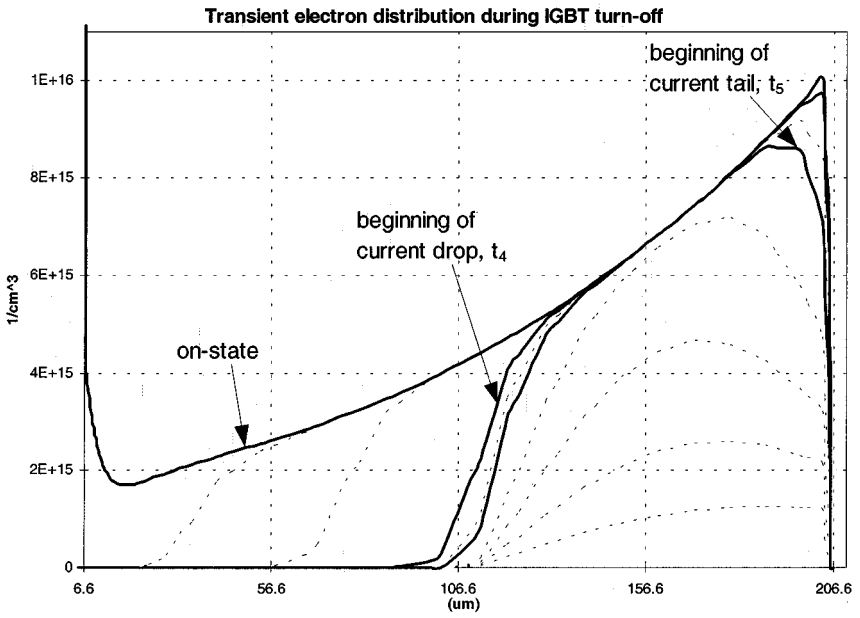

Fig. 3. Transient electron distribution during IGBT turn-off, numerical simulator.

tric field reaches the buffer layer. This phenomena, which is not seen in the semi-mathematical model, is predicted accurately by the Hefner model because of its physics basis. Another pronounced difference between the two models is in the gate waveform. The gate voltage drops from V_{pl} soon after t_3 for the Hefner model (and experimental results) and after t_4 for the semi-mathematical model. Although not affecting the collector waveforms, this difference implies two different internal mechanisms modeling IGBT turn-off. For the semi-mathematical model, the MOS channel current cuts off as the collector current falls while for the Hefner model (and experimentally) cut off occurs as the collector voltage increases. The later condition is correct and can be readily validated by 2-D simulation. (In fact, in deriving the redistribution current of the Hefner model, MOS channel current is set to zero at the commencement of the collector voltage increase). The invalid turn-off mechanism of the semi-mathematical model also causes gross error in the current tail at various DC bus voltage conditions, which can be compensated [51]. The current tail of a PT IGBT (typically less than 0.5 μs at 25°C) is short compared to that of the NPT IGBT which, dependent on technology, can last as long as 40 μs [71].

The analysis above shows that accurate modeling of the gate capacitances and the stored base carrier behavior is important for predicting IGBT hard-switching waveforms.

At turn-on, besides the effects of the associated free-wheeling diode, IGBT gate capacitances (C_{gs}, C_{gd}), threshold voltage (V_{th}) and channel transconductance (K_p) are critical to accurate waveforms.

b) Zero-voltage-switching (ZVS): The use of soft-switching techniques decreases switching losses, EMC and increases maximum switching frequency, but with increased circuit complexity and costs. In this paper Zero-Voltage-Switching (ZVS) refers to the turn-off transient where the device collector current falls before its collector voltage rises because of external circuit configurations [77]. It is called Zero-Current-Switching (ZCS) in some cases [72]. Although there are several different ZVS topologies, their operating conditions at IGBT turn-off are similar to that of switching with a capacitive turn-off snubber.

During a ZVS turn-off transient, the voltage waveform is determined by the external resonant capacitor value and collector current level hence is almost independent of the device. On the other hand, the current waveform is a result of device-circuit interaction. Therefore, only one voltage waveform is shown in Fig. 4 to simplify the graph. The spike at the commencement of the voltage rise is caused by the stray inductance of the device-snubber circuit loop. The device used in this test is an ITE40C06 and its model parameters are shown in Table V in the Appendix. As shown in Fig. 4, current tail behavior changes with changed rate of collector voltage which is controlled by the resonant snubber capacitance. Although the stored charges in the base before switching are the same in each case, the tail current charge for the case with larger parallel capacitance is significantly lower. This shows that tail charge is different from IGBT base stored charge. Accurate simulation of the base charge is important because it dominates current tail behavior. Therefore, more accurate results are obtained with the Hefner model since it includes nonquasi-static carrier redistribution capacitance [9], [11]–[15], [17], [18], [32]. ZVS turn-on behavior is the same as that for a hard-switching circuit at turn-on.

c) Zero-current-switching (ZCS): A turn-on transient where the device voltage falls before its current rises is called Zero-Current-Switching (ZCS). The operating conditions at IGBT turn-on are similar to those of switching with an inductive turn-on snubber. In this circuit, while the current waveform is determined by the external circuit (inductance and rail voltage), the reaction in the voltage waveform depends on the device model. Because of the increasing current, dynamic voltage desaturation occurs, which is higher than the static on-state voltage. This short term higher conduction voltage increases device losses, especially with high frequency operation. It is

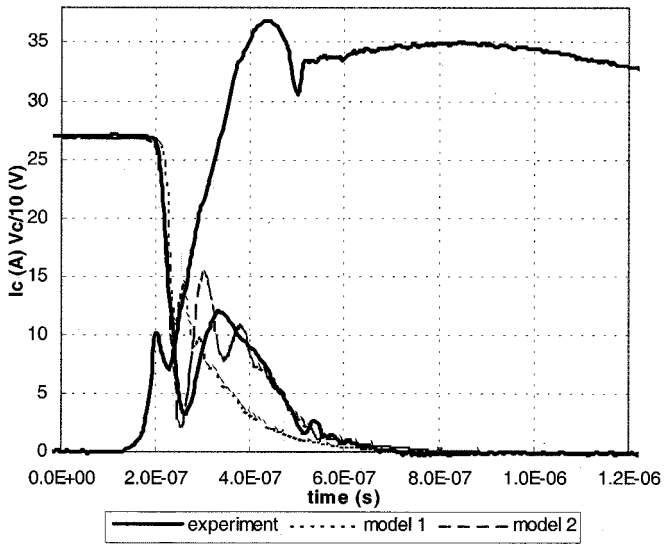

(a)

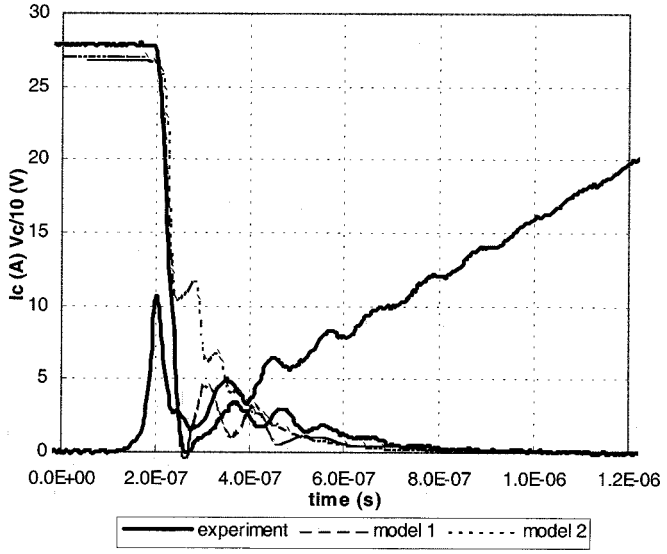

(b)

Fig. 4. Current waveforms at ZVS turn-off for (a) $dv/dt = 1$ kV/μs and (b) $dv/dt = 200$ V/μs.

caused by the base resistance modulation (BRM) lag and device package inductance. Simulation of base-resistance modulation requires accurate parameter values and correct consideration of the IGBT base and its minority carrier distribution. As shown in Fig. 5, without considering BRM, the semi-mathematical model gives less accurate results than the Hefner model. More device oriented analysis of ZCS IGBT turn-on can be found in [74]. The device used in the test is an ITS13C06 and its model parameters are shown in Table V in the Appendix. ZCS turn-off behavior is the same as that for a hard-switching circuit at turn-off.

d) Saturable turn-on snubber switching: The use of a saturable inductor is believed to be better than the use of a linear inductor in reducing turn-on losses [80]. A voltage "bump," as shown in Fig. 6 is induced when the magnetic core saturates and current increases rapidly, which off-sets the benefits. This phenomena can also be found in [74] where no explanation is given. The desaturation voltage bump is caused by BRM lag, packaging inductance and di/dt induced MOS channel turn-off. The later is a result of common emitter inductance which exists in both the power and gate circuit loops. This inductance is negligible for power IGBT modules because of the inclusion of auxiliary emitters. Except for common emitter inductance and BRM, relevant MOS channel parameters, which include gate capacitances (C_{gs}, C_{gd}), threshold voltage (V_{th}) and channel transconductance (K_p), are critical in modeling the voltage waveform in this circuit. Collector voltage behavior with two common emitter inductance values is shown in Fig. 6. Slightly better results are given by the Hefner model. The device used in the test is an IXSH20N60 and its model parameters are shown in Table V in the Appendix. Turn-off behavior is unaffected by the turn-on snubber.

2) Unclamped Inductive Load: Switching with an unclamped inductive load has been studied [9]. Turn-off waveforms of a NPT (BUP304) IGBT with an unclamped inductive load are shown in Fig. 7. The waveforms are similar to those with a clamped inductive load except that lower di/dt and higher voltage over-shoot occur. Both models give accurate results. Besides the gate drive circuitry, gate capacitances (C_{gs}, C_{gd}) and base charge should be modeled correctly to give accurate waveforms [11]. The IGBT collector voltage waveform is linked to the current waveform through the circuit configuration, hence accurate modeling of the first waveform leads to an accurate second waveform.

3) Resistive Load: IGBT turn-off with a resistive load has been discussed extensively [8]. Fig. 8 shows turn-off waveforms for an ultra-fast IGBT (IRG4PC40U) with a resistive load. The initial current drop and the subsequent current tail are not as clearly distinguishable as those in [8], which requires a more accurate model to predict waveforms. Accurate modeling of gate capacitances (C_{gs}, C_{gd}) and base charge are required in order to obtain accurate simulation results. Model parameters used for the IRG4PC40U are shown in Table V in the Appendix.

Modeling parameter requirements for the various circuits discussed above are summarized in the following Table II.

In Table II, the parameters in brackets only affect the gate waveforms significantly. The term C_{cer} refers to carrier redistribution capacitance in the mathematical models and is the output capacitance for semimathematical and behavioral models. The term t_{hl} is carrier high-level injection lifetime in the base for the mathematical models and is the transient time, which dominates tail current decay rate, for semimathematical and behavioral models.

C. Structures

The different technologies result in different structures hence behavior, thus require different models. Two concepts exists for an IGBT vertical structure, namely, punch-through (PT, thin N^- base with an N-buffer) and non-punch-through (NPT, thick N^- base without an N-buffer). PT IGBTs are available in voltage ratings of 500 V, 600 V, 1.2 kV, and 2.5 kV and higher while NPT IGBTs are available at voltage ratings of 600 V, 1 kV, 1.2 kV, 1.6 kV, and 2.5 kV. The structure of the IGBT (PT or NPT) is not considered in all semimathematical and behavioral models in Section II. Therefore they are not able to simulate some of the

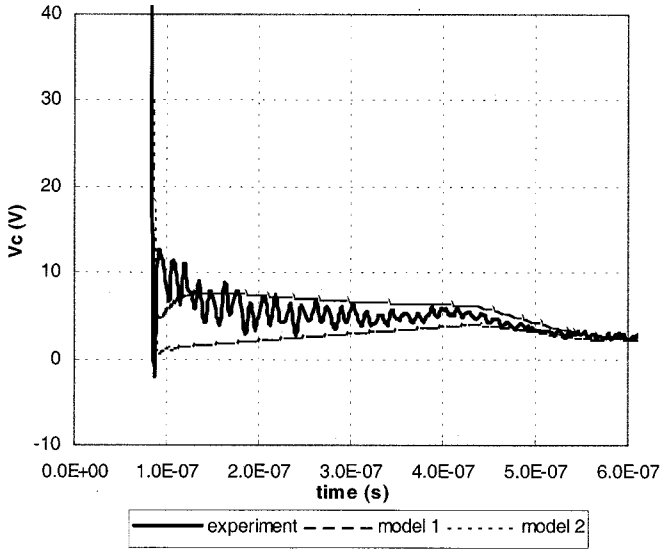

(a)

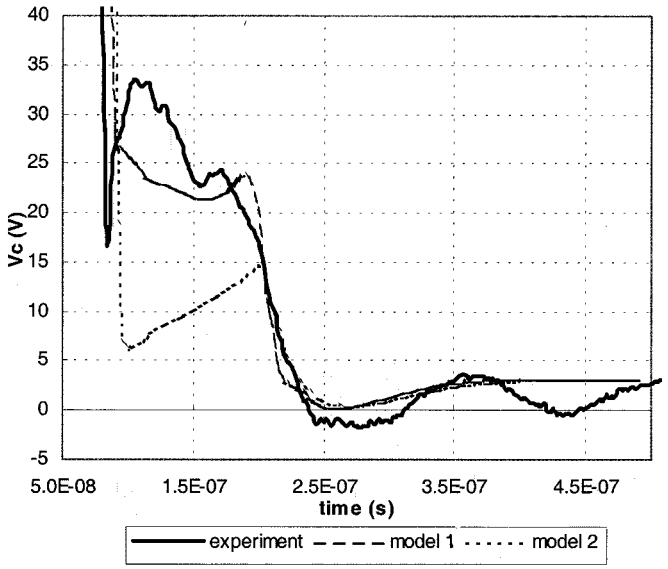

(b)

Fig. 5. Voltage waveforms at ZCS turn-on for (a) $di/dt = 70$ A/μs and (b) $di/dt = 300$ A/μs.

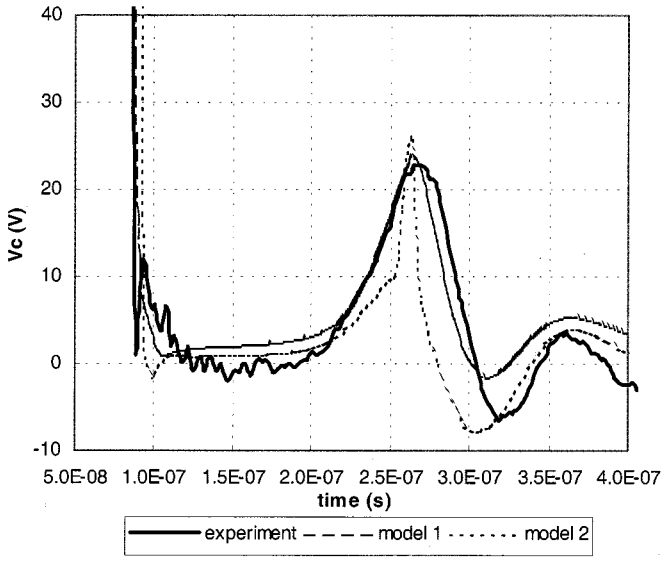

(a)

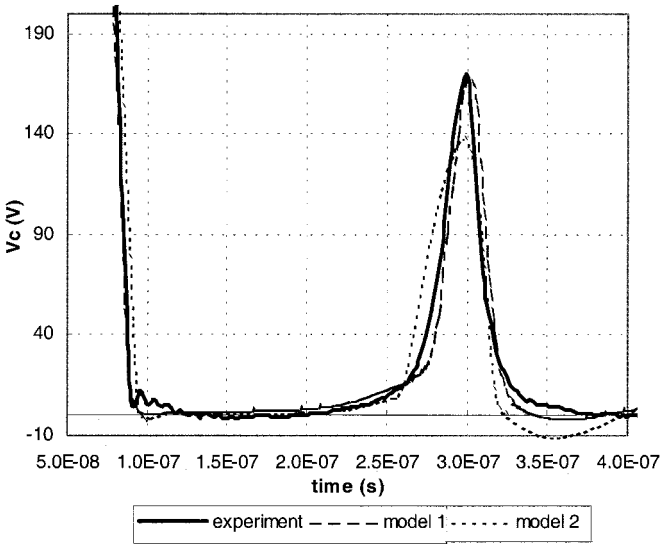

(b)

Fig. 6. Turn-on voltage waveforms with saturable inductor for (a) low L_e and (b) high L_e.

specific phenomena explained in Section III-B, which are associated with the extra buffer layer. Amongst the mathematical and semi-numerical models, some considered both structures: [6], [7], [9], [11]–[15], [17], [18], [32], [42], some are developed only for NPT IGBTs: [19], [24], [25], [33], [34], [36], [39], [44]–[47], [50], [64]–[66], while others are only for PT IGBTs: [35], [60]. With certain simplifications, models in the last category can normally be modified to model NPT IGBTs while extensions are normally required to extend the NPT model to cater for a PT structure. Significant differences on temperature dependence of PT and NPT IGBT behavior will be discussed in the next subsection.

Two structures also exist for the gate, *viz.*, the planar gate structure (DIGBT or DMOS IGBT) and the trench gate structure (TIGBT). Although the TIGBT is superior to the DIGBT in terms of the forward conduction voltage and turn-off losses trade-off, problems associated with short-circuit withstand ability, high voltage oxide reliability and manufacturing costs are currently limiting its development and applications. Therefore, a planar gate is still the dominate IGBT structure. Gate structure is not considered in most of the models listed in Table I. Amongst the models considering 2-D effects, the models in [47], [60] and [66] are developed for the DIGBT, the model in [44], [45], [64] is proposed for the TIGBT while the model in [19] can be used for both structures. Although not considering 2-D effects, the other models listed in Section II can be used for both structures.

D. Temperature Effects

1) Constant Temperature Effects: As a semiconductor device, IGBT behavior is sensitive to operating temperature. Temperature dependant models are useful for the model users to

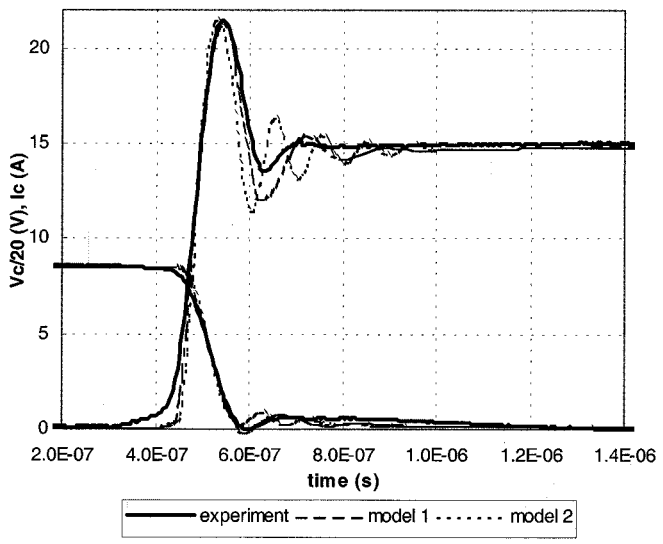

Fig. 7. Turn-off waveforms with an inductive load.

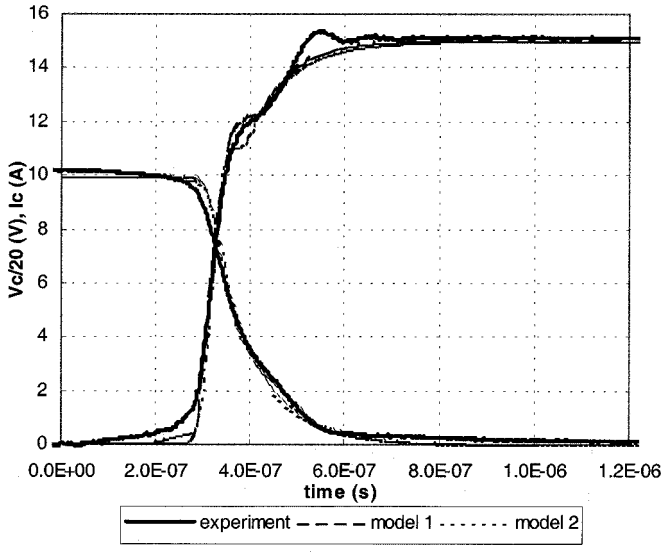

Fig. 8. Turn-off waveforms with a resistive load.

examine the reliability of their designs and devices at elevated temperatures. A room temperature is assumed in many models listed in Table I and high temperature behavior of the models is not discussed. Temperature effects are considered in the models in [21], [23], [25], [33], [34], [40], [49], and [54] by setting the device junction temperature at a certain level during the simulation. It has been shown in [81], [82] that the IGBT junction temperature variation during a normal switching cycle is typically less than two Kelvin, which is readily verifiable with a two dimensional numerical device simulator. Setting a constant junction temperature is therefore acceptable for simulating single cycle switching behavior at the given temperature.

The fact that almost all the basic semiconductor physics parameters are temperature dependent makes it a complicated procedure to consider the temperature dependence of the model. Fortunately, only the temperature dependence of a few parameters needs to be considered to model the temperature dependence of the IGBT behavior, *viz.*, μ_n, μ_p, D_n, D_p, n_i, v_{nsat}, v_{psat}, E_g, τ, V_{th} and K_p [30], [62]. In most of the semi-mathematical models which use existing MOSFET and BJT models, temperature dependencies of some of the parameters mentioned above can be represented by those of the BJT model parameters, e.g., β_f.

The significant difference between temperature dependencies of PT and NPT IGBTs is important for IGBTs. It is well known that, while the on-state voltages of PT IGBTs have a small positive temperature coefficient at typical operating current levels, temperature coefficients of the NPT IGBT on-state voltage is strongly positive. These can be seen in Table III where on-state voltages of a PT (ITH13C06) and a NPT IGBT (BUP304) are modeled with the two models and compared with the experimental results. Both models can account for the difference between on-state voltage temperature dependence of the two structures.

Another important phenomena is that turn-off loss of a PT IGBT is much more sensitive to junction temperature than that of a NPT IGBT, which results in lower high frequency operation reliability for the PT IGBT [82]. Hard-switching turn-off current waveforms of a PT (ITH13C06) and a NPT (BUP304) IGBT are shown in Fig. 9. It is evident from the figure that turn-off loss of the PT IGBT increases significantly at higher temperature while that of the NPT IGBT is almost unchanged. For the PT IGBT, the greatly increased base carrier lifetime at higher temperature results in larger amount of excess base carriers hence the higher and longer tail current. In a NPT IGBT, the low collector injection efficiency together with the already-high base carrier lifetime at the room temperature means that the stored base charge does not increase significantly with temperature. As shown in Fig. 9, both models can account for the temperature dependence of these behaviors.

2) Dynamic Electrothermal Effects: Although the IGBT junction temperature is almost constant during a switching cycle, assuming a constant junction temperature is not valid for simulations involving transient thermal effects. Transient temperature dynamics (self-heating) are important for simulations on short-circuit behavior, high frequency and high temperature operating stability, system thermal behavior at start-up and steady-state, etc. [30] These effects have been included in some of the models in Table I, *viz.*, [24], [50], [30], [62], [58] and [67]. To model the dynamic electrothermal effects, an extra thermal circuit has to be modeled simultaneously with the electrical circuit including the temperature dependent model. The interactions between the two circuits have to be accounted for by calculating the time dependent device junction temperature from the thermal circuit and the power dissipation from temperature dependent device electrical behavior.

As mentioned in the Section III-D1, PT IGBTs are not as stable as NPT IGBTs at high frequencies [82]. Thermal run-away occurs at a lower junction temperature for PT IGBTs than NPT IGBTs, which is an important phenomena for both device manufacturers and circuit designers using IGBTs. These effects can only be modeled by models accounting for the dynamic electrothermal effects.

Another equally important application of the dynamic electrothermal models is to simulate the IGBT short-circuit behavior where the transient device junction temperature plays a crit-

TABLE II
REQUIREMENTS OF AN IGBT MODEL IN DIFFERENT CIRCUIT TOPOLOGIES

circuit conditions	requirements of IGBT model											
	turn-off						turn-on					
Hard-switching, clamped inductive load	C_{cer}	t_{hl}	C_{gd}	C_{gs}	W_b	(V_{th})	C_{gs}	K_p	C_{gd}	(V_{th})		
ZVS, clamped inductive load	C_{cer}	t_{hl}	C_{gd}	C_{gs}		(V_{th})	C_{gs}	K_p	C_{gd}	(V_{th})		
ZCS, clamped inductive load	C_{cer}	t_{hl}	C_{gd}	C_{gs}	W_b	(V_{th})	(C_{gs})				BRM	
Saturable turn-on snubber, clamped inductive load	C_{cer}	t_{hl}	C_{gd}	C_{gs}	W_b	(V_{th})	C_{gs}	K_p		V_{th}	BRM	L_e
Unclamped inductive load	C_{cer}	t_{hl}	C_{gd}	(C_{gs})		(V_{th})	(C_{gs})				BRM	
Resistive load	C_{cer}	t_{hl}	C_{gd}	(C_{gs})		(V_{th})	C_{gs}	K_p	C_{gd}	(V_{th})		

TABLE III
ON-STATE VOLTAGE OF PR AND NPT IGBTS AT DIFFERENT TEMPERATURES

V_{on}@ 15A (V)	PT IGBT			NPT IGBT		
	experiment	model 1	model 2	experiment	mode 1	model 2
27°C	2.5	2.5	2.55	2.8	2.8	2.8
127°C	2.7	2.74	2.6	3.8	3.8	3.8

ical role. Experimental short-circuit waveforms of a PT IGBT (ITS25F12) are shown in Fig. 10 together with those simulated by model 1. Excellent fit between the results has been obtained by accurately simulating both the parasitic circuit components and the IGBT device. In the simulation, a ± 15 V gate drive voltage, a 3 Ω gate resistance, a 16 nH common emitter stray inductance and a 200 nH power loop stray inductance are used. The common emitter stray inductance is dominating the current rise rate at the first stage of the transient while the power loop stray inductance and the di/dt rate determines the voltage waveform. Parameters used in model 1 implemented in Saber are shown in Table V in the Appendix. The most interesting phenomena in the short-circuit waveforms is the decrease of short-circuit current after two microseconds, as shown in Fig. 10. When short-circuited, an IGBT operates in its saturation region (region III in Fig. 1) and the saturation feature of the MOS channel self-limits the short-circuit current to the level of IGBT saturation current. As time elapses, also shown in Fig. 10, the junction temperature of the IGBT increases quickly due to the massive power losses (as high as hundreds of kilo-watts per square centimeter) generated. The reduced channel carrier mobilities at high temperature result in the decreased IGBT saturation current hence decreased short-circuit current. To simulate the IGBT short-circuit behavior correctly, it is therefore necessary to account for the dynamic electro-thermal effect which is included in the models in [24], [50], [30], [62], [58] and [67].

Device failure is an important phenomena of short-circuit test. Successful turn-off of the short-circuit current is shown in Fig. 10. As the short-circuit time increases, the device junction temperature will also increase and device failure will eventually occur. The maximum short-circuit time a device can withstand under certain circumstances is a very important device characteristic. Although it is generally known that decreasing IGBT saturation current hence short-circuit current will increase the IGBT short-circuit withstand ability, insufficient analysis on the maximum short-circuit time of the IGBT is available in the literature. On the failure mechanisms of an IGBT under short-circuit conditions, different analysis and inconsistent results can be found in the literature [83], [84]. Although the exact failure mechanisms have not been concluded, parasitic thyristor latch up is one of the reasons because, at increased temperature, the build-in voltage of the N^+ emitter-P well junction decreases (disappearing at around 650 K [84]) and the device is easier to latch up. Of the four electro-thermal models mentioned above, only the one in [24], [50] included the parasitic latch-up effect hence is able to simulate IGBT short-circuit failure.

E. Simulation Accuracy and Speed

The models listed in Table I have different complexities, accuracies and computational speeds. Model complexity should be selected according to the application requirement, which is summarized in Table IV. Note the models in Table IV shown in italics are not suitable for circuit simulators such as Saber and Spice.

Based on device physics, many mathematical models are accurate and are able to predict electrical behavior in different circuit conditions. In contrast, behavioral models do not normally have forecasting ability because they are based on curve-fitting methods rather than on device physics. The advantage of such models is the shorter development time needed when compared

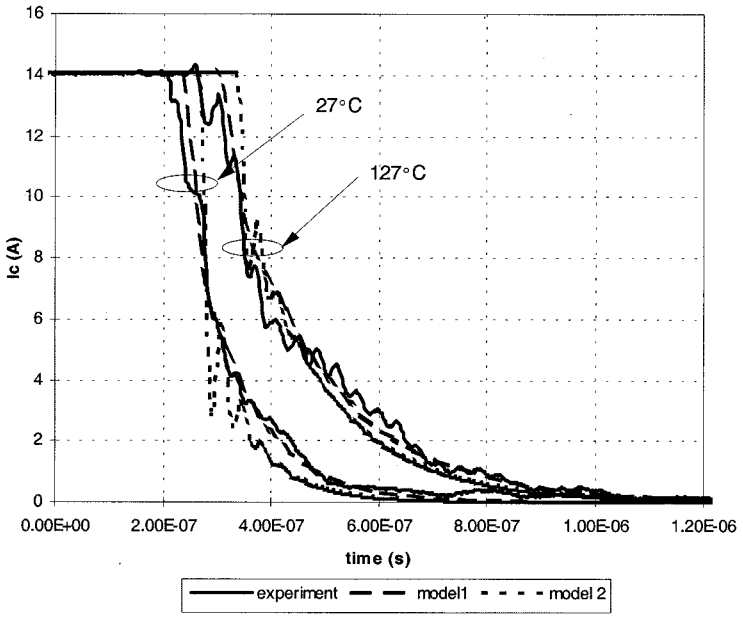

(a)

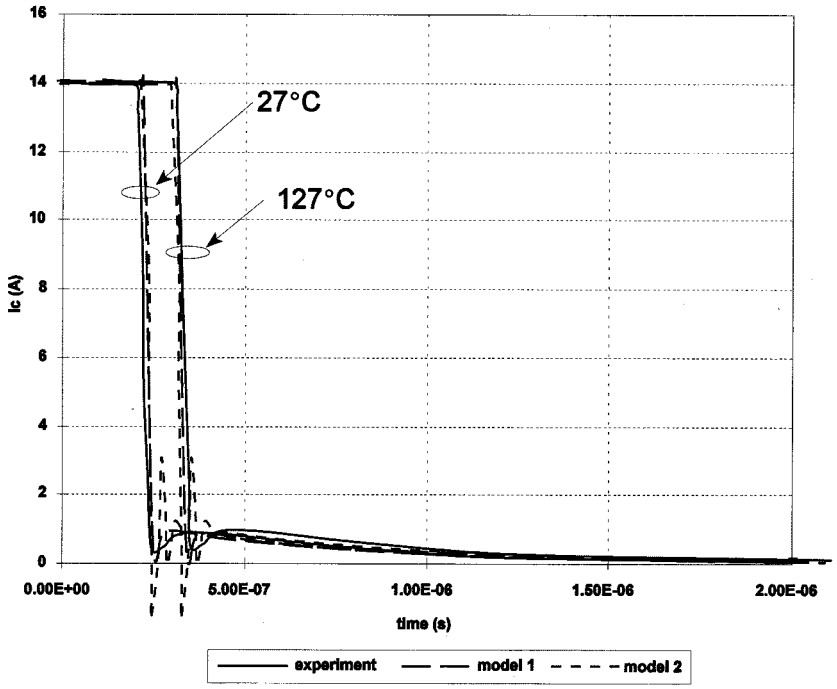

(b)

Fig. 9. Temperature effects on turn-off current waveforms for (a) PT IGBT and (b) NPT IGBT.

with the mathematical models. While the mathematical models are not portable, most semi-mathematical models in Table I are portable amongst various Spice based circuit simulators and Saber. Different models should be selected according to the accuracy and speed required and the application nature.

There is always a trade-off between the speed and the accuracy of an IGBT model. In Table IV, as the model complexity increases down the table, the speed decreases and convergency degrades. However, model type is not the only factor dominating speed and convergency. While the methods and tools used in the model implementation affect model speed slightly, they have a significant effect on convergence. Semiconductor physics equations have difficulty in converging due to wide numerical variations. Various techniques can be used to improve model convergence. Meanwhile, convergency of commercial circuit simulators is improving. Because of their complexity, implementing most mathematical models into subcircuits of a normal circuit simulator like PSpice is inconvenient and may result in poor convergence. A compromise between accuracy and easy of implementation was achieved in [65] where the ambipolar carrier transport equations are implemented into a circuit directly through Laplace transformations. However, for most mathemat-

TABLE IV
MODELS FOR DIFFERENT ACCURACY REQUIREMENTS

Application (increasing complexity)	Required performance	Suitable models
model system performance	very simple, for loss estimation only	*[21]*, [43, 61] and *[54]*
model circuit performance	simple, exhibit basic behaviour without prediction	[22], [43, 61], [57] and [58]

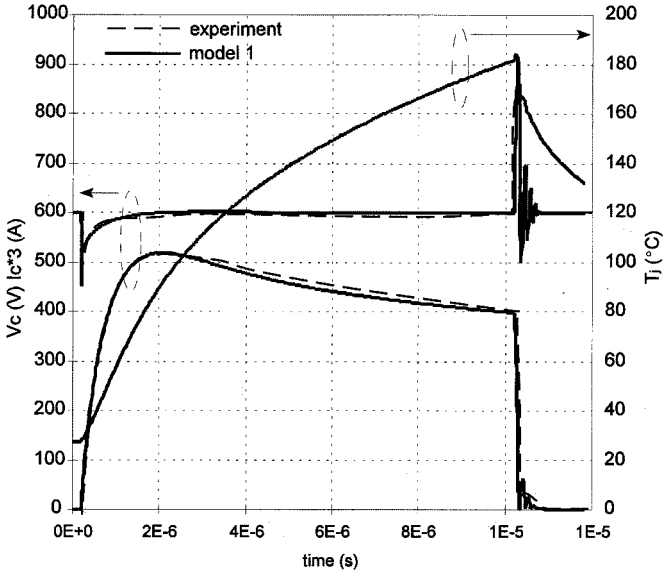

Fig. 10. Short-circuit waveforms of an IGBT.

ical models, being implemented into the source code of a circuit simulator is more robust and effective than subcircuit implementation.

IV. PROBLEMS AND TRENDS

Although satisfactory IGBT models are available for circuit simulation, comprehensive physical models for device mechanism understanding are not. As a bipolar power device, IGBT switching behavior is dominated by the distributed charge in the wide base. Describing the behavior of this charge, which is governed by the ambipolar carrier transport equation (ATE, a second order partial differential equation), is the main challenge in IGBT modeling. In steady state this equation reduces to an ordinary differential equation, and the 1-D solution is used by many of the mathematical models listed in Table I. However, 2-D distribution of carriers in the IGBT base has significant effects on IGBT static characteristics [44], [45], [64], [47], [60] and [66]. These effects are incorporated into the models in [44], [45], [64] and [60]. For dynamic transients, no satisfactory one dimensional analytical solution of the ATE has been obtained. Attempts includes the Hefner model [9], [11]–[15], [17], [18], [30], [32], [42], [62], which is a widely accepted IGBT circuit model, and [19], [24], [50] and [67]. In Fig. 11, the dynamic carrier distribution at NPT IGBT turn-off calculated with the Hefner model is shown. Circuit and device parameters are the same as those used for the two dimensional numerical simulation results in Fig. 3. Significant difference can be seen between Figs. 3–11, which means the Hefner model is inadequate for predicting dynamic carrier behavior, although it is adequate for most circuit simulations. Better results were obtained by Kraus and Hoffmann [19] with a time-varying polynomially approximation. However, the approximation was behavioral, infinite base carrier lifetime was assumed and is difficult to implement into a normal circuit simulator. Neglecting base recombination, an analytical 1-D solution of carrier dynamic distributions was given in [67], which can be used to approximate some NPT IGBTs. Although its validity was not demonstrated, good results can be obtained for the dynamic carrier behavior at turn-on and turn-off voltage rise, with minor modifications to the solution.

In the Hefner model, although the base carrier distribution is solved in steady state, it is inconsistent with the dynamic state distribution. An instantaneous phase change is assumed in the model derivation where the MOS channel current cuts off immediately the turn-off procedure begins.

IGBT short-circuit behavior is important especially for inverter applications where it is most likely to take place. Short-circuit failure behavior has only been modeled in [24], [50]. Because of the lack of analysis on IGBT short-circuit withstand ability limits and the understanding of IGBT short- circuit failure mechanisms, IGBT short-circuit behaviors are not modeled well.

Another limitation aspect is gate capacitances modeling. Large gate capacitance variation for negative gate bias has significant effects on the transient gate waveforms and has only been included in the model in [73]. Negative gate capacitance induced by the accumulation layer under the gate, which might cause instability [78], has not been modeled.

Convergence and speed for most mathematical models are not satisfactory. Although convergence improvements have been made in various circuit simulators, convergence failure still occurs for many applications, particularly more complicated multi-IGBT circuits.

The parameter extraction procedures, which are useful user tools, are not available for many of the models listed in Section II. Parameter extraction procedures are available for the Hefner model, [23], [27], [28], [51], [53], and [67].

V. CONCLUSION

In this paper, IGBT models published in the literature have been reviewed, analyzed, compared and classified into different categories according to mathematical type, objectives, com-

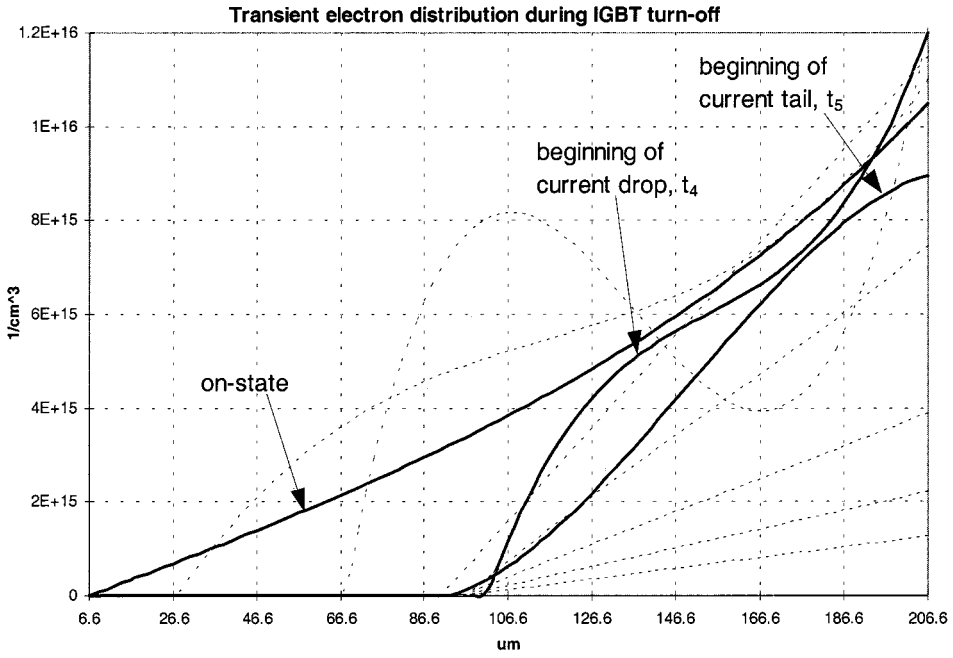

Fig. 11. Transient electron distribution during IGBT turn-off, Hefner model.

TABLE V
MODEL PARAMETERS USED IN THE SIMULATIONS

Device	Model 1	Model 2
IRGP440U	tauhl=8e-8, wb=50m, nb=1.32e14, taubuf=6e-8, wbuf=0.5m, nbuf=2e17, cgs=0.67n, coxd=2n, a=0.4, isne=1f, vt=5.8	PNP(is=4e-14, tf=35n, bf=3, rb=10m) NMOS(cgso=1e-5, cgdo=4e-7, kp=0.8, vto=4.2)
BUP304	tauhl=8u, wb=20m, nb=1e14, cgs=2n, a=0.85, isne=7.5e-12, bvcbo=1000, kp=0.17, isnetexp=2	PNP(tf=10u, bf=0.085, xtb=0.3) NMOS(kp=0.8, cgso=2e-6, cgdo=2e-6, vto=4)
ITE40C06	tauhl=1.8e-7, wb=6.5m, nb=1.3e14, taubuf=9e-8, wbuf=1m, nbuf=5e16, cgs=0.5n, coxd=1n, a=0.3, isne=1f, kp=2	PNP(is=4e-14, tf=60n, bf=1.8) NMOS(cgso=1.2e-5, cgdo=4e-7, kp=0.8, vto=4)
ITE13C06	tauhl=2.3e-7, wb=9.5m, nb=9e13, taubuf=9e-8, wbuf=1m, nbuf=5e16, cgs=0.5n, coxd=1n, a=0.08, isne=1f, kp=2	PNP(tf=90n, bf=0.9, xtb=2.3) NMOS(kp=0.8, cgso=6e-6, cgdo=2e-6, vo=4)
IXSH20N60	tauhl=1.8e-7, wb=9.5m, nb=1e14, taubuf=9e-8, wbuf=1m, nbuf=5e16, cgs=1n, coxd=0.3n, a=0.2, isne=1f, kp=0.37	PNP(is=4e-14, bf=3, rb=10m) NMOS(cgso=1e-6, cgdo=3e-8, kp=1, vto=5, cox=20n)
IRG4PC40U	tauhl=1.8e-7, wb=6.35m, nb=1e14, taubuf=9e-8, wbuf=1m, nbuf=5e16, cgs=1n, coxd=0.3n, a=0.2, isne=1f, kp=0.37	PNP(is=4e-14, tf=28n, bf=3) NMOS(cgso=1e-5, cgdo=4e-7, kp=0.8, vto=4)
ITH13C06	tauhl=9e-8, wb=6.5m, nb=1.3e14, taubuf=9e-8, wbuf=0.6m, nbuf=5e16, taubufexp=2, cgs=1n, coxd=0.41n, a=0.3, agd=0.03, isne=1f	PNP(tf=90n, bf=0.9, xtb=2.3) NMOS(cgso=6e-6, cgdo=2e-6, kp=0.8, vto=4)
ITS25F12	tauhl=1e-7, vttco=4m, kp=0.91, wb=14m, bvcbo=1200, a=0.4, vt=6	N/A

Note: The model parameters are optimized for the application only. Meanings of the symbols used in this table can be found in [85].

plexity, accuracy and speed. Features of the different models are listed. Different modeling criteria have been discussed according to various circuit conditions, structures, thermal considerations and accuracies. Although satisfactory IGBT models are available for various circuit simulations levels, comprehensive physical models for device mechanism understanding are not. Some problems and trends in IGBT modeling were discussed.

APPENDIX

See Table V.

REFERENCES

[1] H. Dettmer, W. Fichtner, F. Bauer, and T. Stockmeier, "Punch-through IGBTs with homogeneous N-base operation at 4 kV line voltage," in *Proc. Int. Symp. Power Semicon. Devices ICs (ISPSD)*, 1995, pp. 492–496.

[2] Databook, European power-semiconductor and electronics company (EUPEC), 1998.

[3] Databook, International Rectifier (IR), 1997.

[4] B. J. Baliga, M. S. Adler, P. V. Gray, R. P. Love, and N. Zommer, "Insulated gate rectifier (IGR): A new power switching device," in *Proc. Tech. Dig. IEDM*, 1982, pp. 264–267.

[5] B. J. Baliag, "Analysis of insulated gate transistor turn-off characteristics," *IEEE Electron Device Lett.*, vol. EDL-6, pp. 74–77, Feb. 1985.

[6] D. S. Kuo, J. Y. Choi, D. Giandomenico, C. Hu, S. P. Sapp, K. A. Sassaman, and R. Bregar, "Modeling the turn-off characteristics of the bipolar-MOS transistor," *IEEE Electron Device Lett.*, vol. EDL-6, pp. 211–214, May 1985.

[7] D. S. Kuo, C. Hu, and S. P. Sapp, "An analytical model for the power bipolar-MOS transistor," *Solid-State Electron.*, vol. 29, no. 12, pp. 1229–1237, 1986.

[8] B. J. Baliga, *Modern Power Devices*. New York: Wiley, 1987, pp. 353–387.

[9] A. R. Hefner, "Analytical modeling of device-circuit interactions for the power insulated gate bipolar transistor (IGBT)," *Conf. Rec.—IAS Annu. Meeting (IEEE Ind. Appl. Soc.)*, vol. 35, no. 6, pp. 606–614, 1988.

[10] J. G. Fossum, R. J. McDonald, and M. A. Shibib, "Network representations of LIGBT structures for CAD of power integrated circuits," *IEEE Trans. Electron Devices*, vol. 35, pp. 507–514, Apr. 1988.

[11] A. R. Hefner, "Improved understanding for the transient operation of the power insulated gate bipolar transistor (IGBT)," in *Proc. PESC Rec.—IEEE Power Electron. Spec. Conf.*, vol. 1, 1989, pp. 303–313.

[12] ——, "An investigation of the drive circuit requirements for the power insulated gate bipolar transistor (IGBT)," in *Proc. PESC Rec.—IEEE Power Electron. Spec. Conf.*, 1990, pp. 126–137.

[13] ——, "Analytical modeling of device-circuit interactions for the power insulated gate bipolar transistor (IGBT)," *IEEE Trans. Ind. Appl.*, vol. 26, pp. 995–1005, Nov./Dec. 1990.

[14] ——, "An investigation of the drive circuit requirements for the power insulated gate bipolar transistor (IGBT)," *IEEE Trans. Power Electron.*, vol. 6, pp. 208–219, Apr. 1991.

[15] ——, "An improved understanding for the transient operation of the power insulated gate bipolar transistor (IGBT)," *IEEE Trans. Power Electron.*, vol. 5, pp. 459–468, Oct. 1990.

[16] Z. Shen and T. P. Chow, "An analytical IGBT model for power circuit simulation," in *Proc. 3rd Int. Symp. Power Semicond. Devices ICs ISPSD*, 1991, pp. 79–82.

[17] C. S. Mitter, A. R. Hefner, D. Y. Chen, and F. C. Lee, "Insulated gate bipolar transistor (IGBT) modeling using IG-SPICE," in *Proc. 91 IEEE Ind. Appl. Soc. Annu. Meeting*, 1992, pp. 1515–1521.

[18] A. R. Hefner and D. M. Diebolt, "An experimentally verified IGBT model implemented in the Saber circuit simulator," in *Proc. PESC Rec.—IEEE Power Electron. Spec. Conf.*, 1991, pp. 10–19.

[19] R. Kraus and K. Hoffmann, "Analytical model of IGBTs with low emitter efficiency," in *Proc. Int. Symp. Power Semicond. Devices ICs*, 1993, pp. 30–34.

[20] Z. Shen and R. P. Chow, "Modeling and characterization of the insulated gate bipolar transistor (IGBT) for SPICE simulation," in *Proc. BN: Int. Symp. Power Semicond. Devices ICs*, 1993, pp. 165–170.

[21] S. M. Clemente and D. A. Dapkus, "IGBT models account for switching and conduction losses," *Power Conv. Intell. Motion*, vol. 19, no. 8, pp. 51–54, Aug. 1993.

[22] Y. Y. Tzou and L. J. Hsu, "Practical SPICE macro model for the IGBT," *IECON Proc. (Ind. Electron. Conf.)*, vol. 2, pp. 762–766, 1993.

[23] F. F. Protiwa, O. Apeldoorn, and N. Groos, "New IGBT model for PSpice," *IEE Conf. Publ.*, vol. 2, no. 377, pp. 226–231, 1993.

[24] B. Fatemizadeh and D. Silber, "A versatile electrical model for IGBT including thermal effects," in *Proc. PESC Rec.—IEEE Annu. Power Electron. Spec. Conf.*, 1993, pp. 85–92.

[25] D. Metzner, "Modular concept for the circuit simulation of bipolar power semiconductors," *IEE Conf. Publ.*, vol. 2, no. 377, pp. 15–20, 1993.

[26] O. Kvien, T. M. Undeland, and T. Rogne, "Models for simulation of diode (and IGBT) switchings which include the effect of the depletion layer," in *Proc. Conf. Rec.—IAS Annu. Meeting (IEEE Ind. Appl. Soc.)*, vol. 2, 1993, pp. 1190–1195.

[27] H. S. Kim, Y. H. Cho, S. D. Kim, Y. I. Choi, and M. K. Han, "Parameter extraction for the static and dynamic model of IGBT," Tech. Rep., 1993.

[28] M. Andersson, P. Kuivalainen, and H. Pohjonen, "Circuit simulation models for MOS-gated power devices: Application to the simulation of an electronics lamp ballast circuit," in *Proc. Conf.—IEEE Applicat. Power Electron. Expo—APEC*, 1993, pp. 498–503.

[29] J. M. Li, D. Lafore, J. Arnould, and B. Reymond, "Analysis of switching behavior of the power insulated gate bipolar transistor by soft modeling," in *Proc. EPE'93*, 1993, pp. 220–225.

[30] A. R. Hefner, "Dynamic electro-thermal model for the IGBT," *IEEE Trans. Ind. Applicat.*, vol. 30, pp. 364–405, Mar./Apr. 1994.

[31] J. B. Kuo and C. S. Chiang, "Turn-on transient analysis of a power IGBT with an inductive load in series with a resistive load," *Solid-State Electron.*, vol. 37, no. 9, pp. 1673–1676, Sept. 1994.

[32] A. R. Hefner and D. M. Diebolt, "Experimentally verified IGBT model implemented in the Saber circuit simulator," *IEEE Trans. Power Electron.*, vol. 9, pp. 532–542, Sept. 1994.

[33] D. Metzner, T. Vogler, and D. Schroeder, "Modular concept for the circuit simulation of bipolar power semiconductors," *IEEE Trans. Power Electron.*, vol. 9, pp. 506–513, Sept. 1994.

[34] H. Goebel, "Unified method for modeling semiconductor power devices," *IEEE Trans. Power Electron.*, vol. 9, pp. 497–505, Sept. 1994.

[35] V. A. Kuzmin, S. N. Yurkov, and L. I. Pomortseva, "Analysis and simulation of insulated gate bipolar transistor with buffer N'-layer," in *Proc. IEE Conf. Publ., Power Electron. Variable-Speed Drives*, vol. 399, 1994, pp. 24–28.

[36] B. Allard, H. Morel, C. C. Lin, H. Helali, and J. P. Chante, "Rules for deriving basic semiconductor region models," in *Proc. PESC Rec.—IEEE Annu. Power Electron. Spec. Conf.*, 1994, pp. 44–51.

[37] D. Kovac and I. Kovacova, "New switching simulation models of power electronic parts as IGBT, MOSFET and power diode," *IECON Proc. (Ind. Electron. Conf.)*, vol. 1, pp. 124–128, 1994.

[38] K. Besbes, "Modeling an insulated gate bipolar transistor using bond graph techniques," *Int. J. Numer. Modeling: Electron. Networks, Devices Fields*, vol. 8, no. 1, pp. 51–60, Jan./Feb. 1995.

[39] P. Spanik, B. Dobrucky, and R. Gubric, "Dynamic modeling of IGBT with reverse diode modeling," *Meas. Contr. A: General Phys., Electron., Electr. Eng.*, vol. 59, no. 1–3, pp. 23–32, 1995.

[40] F. Mihalic, K. Jezernik, D. Krischan, and M. Rentmeister, "IGBT SPICE model," *IEEE Trans Ind. Electron.*, vol. 42, pp. 98–105, Feb. 1995.

[41] C. Alonso and T. A. Meynard, "Simulation of short-circuit phenomena in IGBT," in *Proc. IEE Colloq. (Dig.)*, 1994, p. 10/1–5.

[42] A. R. Hefner, "Modeling buffer layer IGBTs for circuit simulation," *IEEE Trans. Power Electron.*, vol. 10, pp. 111–123, Mar. 1995.

[43] C. Wong, "EMTP modeling of IGBT dynamic performance for power dissipation estimation," in *Proc. Conf. Rec.—IAS Annu. Meeting (IEEE Ind. Applicat. Soc.)*, vol. 3, 1995, pp. 2656–2662.

[44] F. Udrea and G. A. J. Amaratunga, "A unified analytical model for carrier dynamics in trench insulated gate bipolar transistor (TIGBT)," in *Proc. IEEE Int. Symp. Power Semiconductor Devices ICs (ISPSD)*, 1995, pp. 190–200.

[45] ——, "Steady-state analytical model the trench insulated gate bipolar transistor," in *Proc. Int. Semiconductor Conf., CAS*, 1995, pp. 49–52.

[46] L. Sabesan, P. Mawby, M. Towers, K. Board, and P. Waind, "Analysis of nonpunch through trench emitter insulated gate bipolar transistor (IGBT)," in *Proc. IEEE Region 10 Annu. Int. Conf./TENCON*, 1995, pp. 420–423.

[47] W. Feiler, W. Gerlach, and U. Wiese, "Two-dimensional analytical models of the carrier distribution in the on-state of the IGBT," *Solid-State Electron.*, vol. 38, no. 10, pp. 1781–1790, 1995.

[48] Y. Kawaguchi, Y. Terazaki, and A. Nakagawa, "Subcircuit spice modeling of a lateral IGBT for high voltage power IC design," in *Proc. 1995 Int. Symp. Power Semicond. Devices ICs*, 1995, pp. 346–349.

[49] A. F. Petrie and C. Hymowitz, "SPICE model accurately simulates IGBT parameters," *Power Conversion Intell. Motion*, vol. 22, no. 1, pp. 40–51, Jan. 1996.

[50] B. Fatemizadeh, G. Tchouangue, and D. Silber, "User-optimized electro-thermal IGBT model for power electronic circuit simulation in the circuit simulator ELDO," in *Proc. IEEE Appl. Power Electron. Conf. Expo—APEC*, vol. 1, 1996, pp. 81–87.

[51] S. Musumeci, A. Raciti, M. Sardo, F. Frisina, and R. Letor, "PT-IGBT PSpice model with new parameter extraction for life-time and epy dependent behavior simulation," in *Proc. PESC Rec.—IEEE Annu. Power Electron. Spec. Conf.*, vol. 2, 1996, pp. 1682–1688.
[52] A. Agbossou, I. Rasoanarivo, and B. Davat, "Comparative study of high power IGBT model behavior in voltage source inverter," in *Proc. PESC Rec.—IEEE Annu. Power Electron. Specialists Conf.*, vol. 1, 1996, pp. 56–61.
[53] J. T. Hsu and K. D. T. Ngo, "Behavioral modeling of the IGBT using the Hammerstein configuration," *IEEE Trans. Power Electron.*, vol. 11, pp. 746–754, Nov. 1996.
[54] F. Blaabjerg, F. K. Pedersen, S. Sigurjonsson, and A. Elkjaer, "Extended model of power losses in hard-switched IGBT-inverters," in *Proc. Conf. Rec.—IAS Annu. Meeting (IEEE Ind. Applicat. Soc.)*, vol. 3, 1996, pp. 1454–1463.
[55] K. Sheng, S. J. Finney, and B. W. Williams, "Fast and accurate IGBT model for PSpice," *Electron. Lett.*, vol. 32, no. 25, pp. 2294–2295, Dec. 5, 1996.
[56] A. Monti, "Fuzzy-based black-box approach to IGBT modeling," in *Proc. IEEE Int. Conf. Electron., Circuits, Syst.*, vol. 2, 1996, pp. 1147–1150.
[57] L. Zhang, C. Watthanasarn, and W. Shepherd, "IGBT modeling using HSPICE," in *Proc. Int. Power Electron. Congr.—CIEP*, 1996, pp. 160–169.
[58] A. Amimi, R. Bouchakour, and T. Maurel, "Modeling of self-heating and degradation effects on the electrical behavior of the IGBT," in *Proc. PEMC'96*, vol. 1, 1996, pp. 146–150.
[59] Y. Yue, J. J. Liou, and I. Batarseh, "Steady-state and transient IGBT model valid for all free-carrier injection conditions," in *Proc. IEEE Appl. Power Electron. Conf. Expo—APEC*, vol. 1, 1997, pp. 168–174.
[60] K. Sheng, S. J. Finney, and B. W. Williams, "A new analytical IGBT model with improved electrical characteristics," *IEEE Trans. Power Electron.*, vol. 14, pp. 98–107, Jan. 1999.
[61] C. Wong, "EMTP modeling of IGBT dynamic performance for power dissipation estimation," *IEEE Trans. Ind. Applicat.*, vol. 33, pp. 64–71, Jan./Feb. 1997.
[62] H. A. Mantooth and A. R. Hefner, "Electrothermal simulation of an IGBT PWM inverter," *IEEE Trans. Power Electron.*, vol. 12, pp. 474–484, May 1997.
[63] R. Sunkavalli and B. J. Baliga, "Analysis of on-state carrier distribution in the DI-LIGBT," *Solid-State Electron.*, vol. 41, no. 5, pp. 733–738, May 1997.
[64] F. Udrea and G. A. J. Amaratunga, "On-state analytical model for the trench insulated gate bipolar transistors (TIGBT)," *Solid-State Electron.*, vol. 41, no. 8, pp. 1111–1118, Aug. 1997.
[65] A. G. M. Strollo, "New IGBT circuit model for SPICE simulation," in *Proc. PESC Rec.—IEEE Annu. Power Electron. Spec. Conf.*, vol. 1, 1997, pp. 133–138.
[66] E. Napoli, A. G. M. Strollo, and P. Spirito, "Two-dimensional modeling of on state voltage drop in IGBT," in *Proc. Int. Conf. Microelectron.*, vol. 2, 1997, pp. 505–508.
[67] J. Sigg, P. Tuerkes, and R. Kraus, "Parameter extraction methodology and validation for an electro-thermal physics-based NPT IGBT model," in *Proc. Conf. Rec.—IAS Annu. Meeting (IEEE Ind. Applicat. Soc.)*, vol. 2, 1997, pp. 1166–1173.
[68] A. Ammous, B. Allard, and H. Morel, "Transient temperature measurements and modeling of IGBTs under short circuit," *IEEE Trans. Power Electron.*, vol. 13, pp. 12–25, Jan. 1998.
[69] Y. Kim and J. G. Fossum, "Physical DMOST modeling for high-voltage IC CAD," *IEEE Trans. Electron Devices*, vol. 37, pp. 797–803, Mar. 1990.
[70] I. K. Budihardjo, P. O. Lauritzen, and H. A. Mantooth, "Performance requirements for power MOSFET models," *IEEE Trans. Power Electron.*, vol. 12, pp. 36–45, Jan. 1997.
[71] J. Yamashita, T. Yamada, S. Uchida, H. Yamaguchi, and S. Ishizawa, "A relation between dynamic saturation characterisitcs and tail current of nonpunch-through IGBT," in *Proc. Conf. Rec.—IAS Annu. Meeting (IEEE Ind. Applicat. Soc.)*, 1996, pp. 1425–1432.
[72] S. Lefebvre, F. Forest, and J. P. Chante, "Maximum switching frequency choice for the IGBT used in ZCS mode," in *Proc. Eur. Power Electron. Conf. (EPE)*, 1993, pp. 356–361.
[73] Y. Lembeye, J. L. Schanen, and J. P. Keradec, "Experimental characterization of insulated gate power components: Capacitive aspects," in *Proc. Conf. Rec.—IAS Annu. Meeting (IEEE Ind. Applicat. Soc.)*, vol. 2, 1997, pp. 983–988.
[74] M. Trivedi and K. Shenai, "Critical evaluation of IGBT performance in zero current switching environment," in *Proc. Conf. Rec.—IAS Annu. Meeting (IEEE Ind. Applicat. Soc.)*, vol. 2, 1997, pp. 989–993.
[75] I. Widjaja, A. Kurnia, K. Shenai, and D. M. Divan, "Switching dyanmics of IGBTs in soft-switching converters," *IEEE Trans. Electron Devices*, vol. 42, pp. 445–454, Mar. 1995.
[76] T. Nilsson, "The insulated gate bipolar transistor response in different short circuit situations," in *Proc. Eur. Power Electron. Conf. (EPE)*, 1993, pp. 328–331.
[77] A. Elasser, M. J. Schutten, V. Vlatkovic, D. A. Torrey, and M. H. Kheraluwala, "Switching losses of IGBTs under zero-voltage and zero-current switching," in *Proc. PESC Rec.—IEEE Annu. Power Electron. Spec. Conf.*, 1996, pp. 600–607.
[78] I. Omura and W. Fichtner, "IGBT instability due to negative gate capacitance," in *Proc. Eur. Power Electron. Conf. (EPE)*, vol. 2, 1997, pp. 66–69.
[79] K. Sheng, S. J. Finney, B. W. Williams, X. N. He, and Z. M. Qian, "IGBT switching losses," in *Proc. 2nd Int. Conf. Power Electron. Motion Contr.*, vol. 1, Hangzhou, China, pp. 274–277.
[80] B. W. Williams, *Power Electronics*, 2nd ed. New York: MacMillan, 1992.
[81] S. Clemente, "Transient thermal response of power semiconductors to short power pulses," *IEEE Trans. Power Electron.*, vol. 8, pp. 337–341, Mar. 1993.
[82] K. Sheng, S. J. Finney, and B. W. Williams, "Thermal stability of IGBT high frequency operation," *IEEE Trans. Ind. Electron.*, vol. 47, pp. 1–16, Feb. 2000.
[83] M. Trivedi and K. Shenai, "Investigation of the short-circuit performance of an IGBT," *IEEE Trans. Electron Devices*, vol. 45, pp. 313–320, Feb. 1998.
[84] H. Hagino, J. Yamashita, A. Uenishi, and H. Haruguchi, "An experimental and numerical study on the forward biased SOA of IGBTs," *IEEE Trans. Electron Devices*, vol. 43, pp. 490–499, June 1996.
[85] *Saber Manual*. New York: Analogy, Inc., 1996.

Kuang Sheng was born in Zhejiang Province, China, in 1974. He received the B.Sc. degree from Zhejiang University, China, in 1995 and the Ph.D. degree from Heriot-Watt University, U.K., in 1999, both in electrical engineering.

He is a Research Associate in the Engineering Department, Cambridge University, Cambridge, U.K. His research interests include design, modeling, and application of power semiconductor devices, new materials for power devices, power integrated circuit, device-circuit interaction, and power electronics circuit techniques.

Barry W. Williams received the M.Eng.Sc. degree from the University of Adelaide, Adelaide, Australia, in 1978 and the Ph.D. degree from Cambridge University, Cambridge, U.K., in 1980.

After seven years as a Lecturer at Imperial College, University of London, London, U.K., he was appointed to a Chair of Electrical Engineering at Heriot-Watt University, Edinburgh, U.K., in 1986. His teaching covers power electronics (in which he has a text published) and drive systems. His research activity includes power semiconductor modeling and protection, converter topologies and soft-switching techniques, and application of ASICs and microprocessors to industrial electronics.

Stephen J. Finney received the M.Eng. degree from Loughborough University of Technology, Loughborough, U.K., in 1988 and the Ph.D. degree from Heriot-Watt University, Edinburgh, U.K.

He worked for two years for the Electricity Council Research Centre Laboratories, Chester, U.K., and is now a Lecturer with Heriot-Watt University. His areas of interest are soft-switching techniques, power semiconductor protection, energy recovery snubber circuits, and low distortion rectifier topologies.